

Acknowledgements

We thank A. G. Navarro-Sigüenza, J. E. Llorente-Bousquets, A. M. Luis, I. Vargas and L. Oniate for assembling distributional data, C. Thomas for help and advice, and E. Martínez-Meyer, G. Jiménez-Casas, S. Egbert and K. P. Price for collaboration. This research was supported by the US National Science Foundation, and grants from CONACyT and DGAPA to J. Soberón and V. Sánchez-Cordero.

Competing interests statement

The authors declare that they have no competing financial interests.

Correspondence and requests for materials should be addressed to A.T.P. (e-mail: town@ukans.edu).

Extraction of a weak climatic signal by an ecosystem

Arnold H. Taylor^{*†}, J. Icarus Allen^{*} & Paul A. Clark[‡]

^{*} Plymouth Marine Laboratory, Prospect Place, Plymouth PL1 3DH, UK

[†] Department of Mathematics and Statistics, University of Plymouth, Plymouth, UK

[‡] Department of Geography, University of Sussex, Brighton BN1 9SJ, UK

The complexity of ecosystems can cause subtle¹ and chaotic responses to changes in external forcing². Although ecosystems may not normally behave chaotically³, sensitivity to external influences associated with nonlinearity can lead to amplification of climatic signals. Strong correlations between an El Niño index and rainfall and maize yield in Zimbabwe have been demonstrated⁴; the correlation with maize yield was stronger than that

with rainfall. A second example is the 100,000-year ice-age cycle, which may arise from a weak cycle in radiation through its influence on the concentration of atmospheric CO₂ (ref. 5). Such integration of a weak climatic signal has yet to be demonstrated in a realistic theoretical system. Here we use a particular climatic phenomenon—the observed association between plankton populations around the UK and the position of the Gulf Stream^{6,7}—as a probe to demonstrate how a detailed marine ecosystem model extracts a weak signal that is spread across different meteorological variables. Biological systems may therefore respond to climatic signals other than those that dominate the driving variables.

Figure 1 illustrates this relationship with the latitude of the Gulf Stream (the GSNW index^{6,7}) at five locations in the North Sea over a period of three decades using zooplankton data collected by the Continuous Plankton Recorder Survey⁸, together with zooplankton data from a site off the Northumberland coast⁹. These are expressed as cumulative sums of the square of the difference between the zooplankton and GSNW index series after each series has been converted to a mean of zero and unit standard deviation¹⁰. Cumulative sums provide a sensitive test of whether the relationship is constant with time. When the variables are positively correlated the slope of the graph will be close to zero, rising to 2.0 if the variables are uncorrelated. In the central and southern North Sea abrupt changes in slope show that the relationship has not been constant with time. Figure 1 also shows data for a freshwater lake in the north of England, Esthwaite water¹¹, and similar results have been obtained in a neighbouring lake, Windermere¹². The probabilities that slopes such as these might arise by chance (see Methods section) are also shown in Fig. 1. Similar probabilities calculated using the North Atlantic Oscillation (NAO) index¹³ instead of the GSNW index were much higher and all were over 0.1, showing that the GSNW teleconnection is distinct from the effects of the NAO.

In order to determine how the GSNW signal finds its way into the plankton, time series of hourly surface heat fluxes calculated from

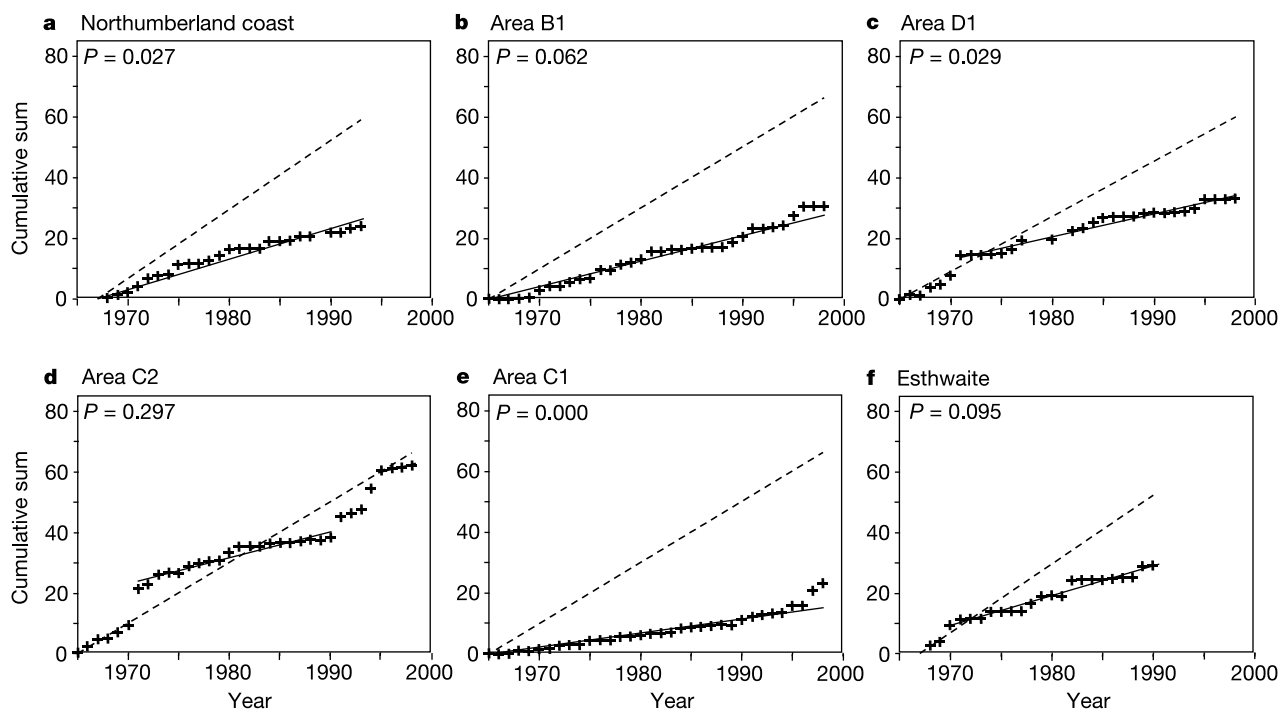


Figure 1 Correlation of observed plankton populations in and around the UK with the latitude of the Gulf Stream. Cumulative sum of the square of the difference between the abundance of total copepods and the GSNW index (crosses) at a site off the coast of Northumberland; in northern (B1), central (C1 and C2) and southern (D1) areas of the

North Sea and in Esthwaite water, UK (using *Daphnia* instead of total copepods). The solid lines are regression fits (included only to highlight the linear parts) and the broken lines show the results for an uncorrelated pair of time-series. The probabilities *P* that the slopes arose by chance are shown.

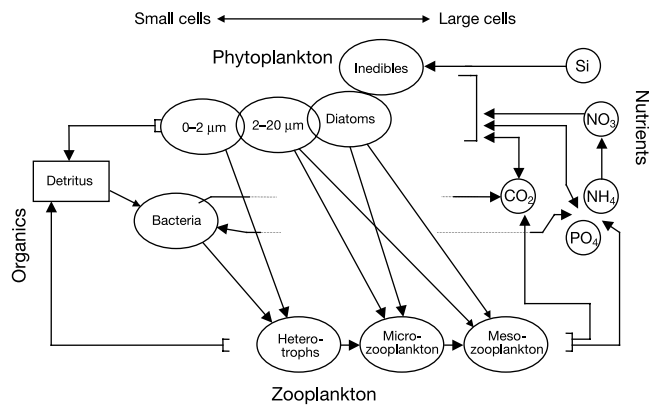


Figure 2 Trophic structure of the pelagic components of the ERSEM ecosystem model. See Methods for details.

meteorological observations made at Dublin from 1966 to 1998 were used to drive a coupled physical–ecological water-column model^{14,15}. This model is a synthesis of the European Regional Seas Ecosystem Model (ERSEM)¹⁶ with a one-dimensional version of the Princeton Ocean Model (POM)¹⁷. Details of the model are given in the Methods section and Fig. 2. The simulations are of a generic, seasonally stratified water column typical of the northern North Sea and as such may be representative of the areas in Fig. 1.

The solid lines in Fig. 3 show cumulative sum plots calculated for six of the variables from time series of April–September means produced by the model. Five of these graphs—the abundances of mesozooplankton (Fig. 3a), heteroflagellates (Fig. 3c) and total phytoplankton carbon (Fig. 3d), and the rates of total primary production (Fig. 3e) and bacteria uptake of inorganic nitrogen (Fig. 3f)—show a prolonged period through the 1970s and 1980s

when the slope was considerably less than the random value of 2, with graphs similar to those presented in Fig. 1. The probabilities of these occurring in random data was less than 0.05 in each case. This pattern is widespread in the ERSEM output. When the probabilities were calculated for 25 of the major standing stocks and fluxes, 19 were 0.1 or less. If the variables were independent such frequencies would only be expected to occur much less than once in a thousand times by chance. The variables in ERSEM are not, of course, independent. When principal components analysis was applied to the 25 time series it was found that 8 variables accounted for 98% of the total variance. If the degrees of freedom are reduced proportionally the frequencies would still occur by chance less than 1 in 20 times. As in the data of Fig. 1, these relationships are not just the effect of the NAO; using the NAO index instead of the GSNW index raises the 25 probabilities from an average of 0.11 to one of 0.32, even though the NAO is possibly the most important constituent of the meteorological observations¹³.

Analysis of the meteorological observations reveals that the GSNW signal is scattered through the data rather than localized in any particular subset. Cumulative sum plots and probabilities calculated from seasonal values of the main atmospheric driving variables—insolation and wind-strength—are shown in Fig. 4a and b. All of these graphs, apart from the wind strength in winter, have probabilities of well over 0.1, implying that the GSNW signal is only a weak constituent of these atmospheric data. These probabilities are much larger than those obtained from the ERSEM output. This relative weakness of the signal in the meteorological observations has been noted previously^{7,18}.

The way in which this weak signal comes to appear in the ERSEM output can be illustrated by comparing the model results in Fig. 3 with the other graphs on the figure in which either the insolation or the wind strength was fixed at its mean annual cycle. Four of the variables—total phytoplankton carbon (Fig. 3d), total primary production (Fig. 3e), bacterial nitrogen uptake (Fig. 3f) and

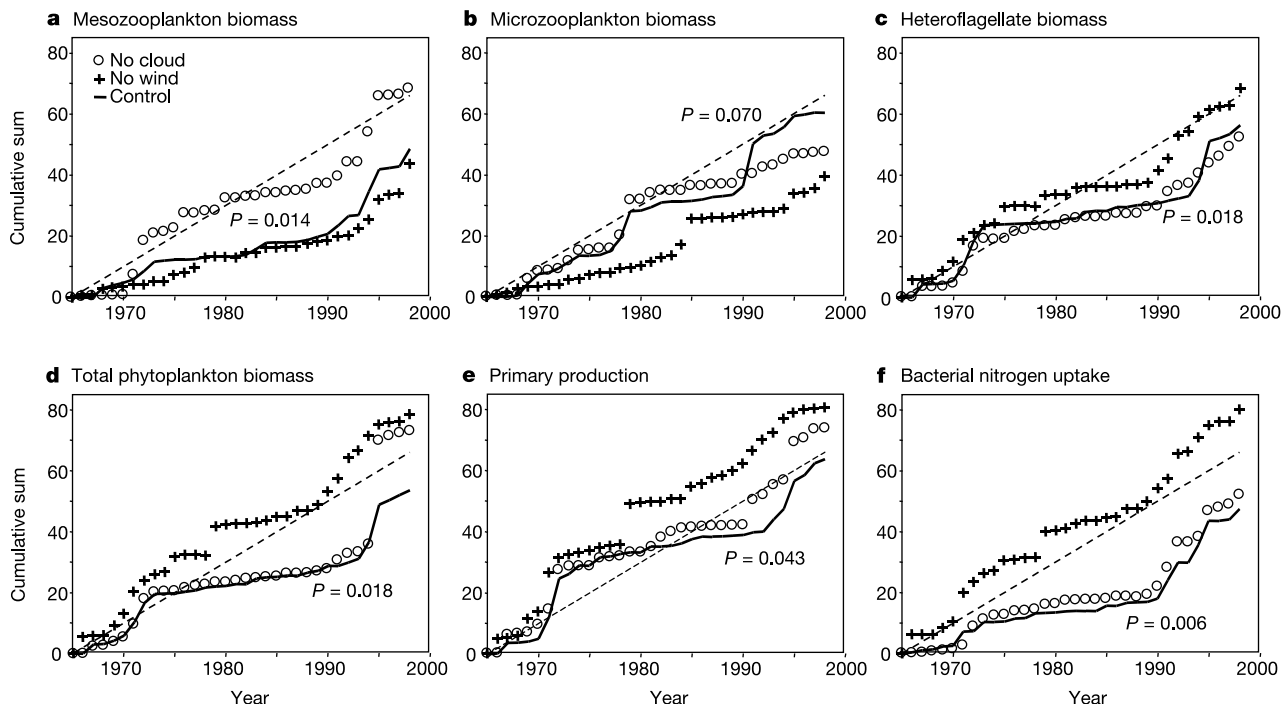


Figure 3 Correlation of simulated plankton populations with the latitude of the Gulf Stream. Cumulative sum of the square of the difference between the predicted time series of mean summer values (April to September) obtained from a run of the ERSEM model for 1966 to 1998 and the GSNW index. Plots (solid lines) are shown for the abundance of mesozooplankton, microzooplankton, heteroflagellates and all phytoplankton, the total

rate of primary production and the ammonium uptake by bacteria from the control run. The broken lines show the results for an uncorrelated pair of time-series. The circles and the crosses show the results when interannual variations were removed from the incident irradiance (no cloud) and the wind strength (no wind), respectively.

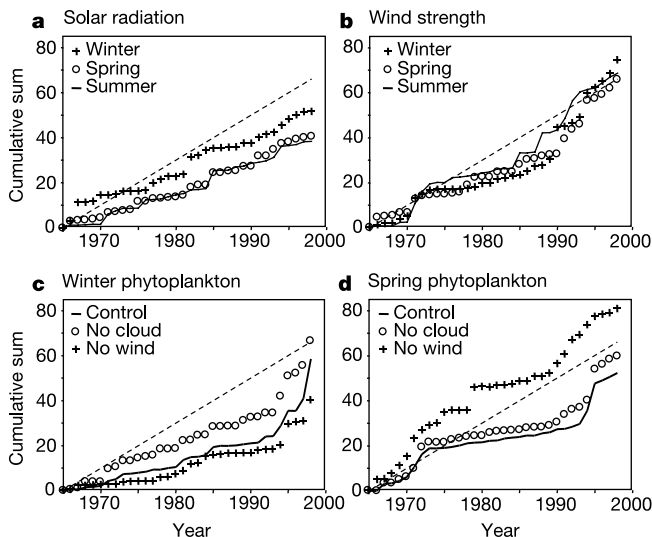


Figure 4 Correlation of meteorological forcing and phytoplankton populations with the latitude of the Gulf Stream. Cumulative sum of the square of the difference between the GSNW index and averages over winter (crosses), spring (circles) and summer (solid line) of solar irradiance (a) and wind strength (b), and averages over winter (c) and spring (d) of total phytoplankton abundance predicted by ERSEM. In c and d the solid line shows the standard model run, and the circles and crosses indicate those when interannual variations were removed from the incident irradiance and the wind strength, respectively. The broken lines show the results for an uncorrelated pair of time-series.

heterotrophic flagellate abundance (Fig. 3c)—show very little change when interannual variability is removed from the solar radiation, but have a random relationship with the GSNW index when the variability is removed from the wind strength. Over the summer period, means of these variables will be dominated by nutrient limitation when fluctuations in the supply of nutrients associated with changes in windiness are important. In contrast, the GSNW signal in the mesozooplankton is much more dependent on the radiation changes than on the wind variations and it is the non-varying insolation results that are close to the random line. Micro-zooplankton, which graze on the phytoplankton and heteroflagellates and which are preyed on by the mesozooplankton, show a more complex relationship resulting from both top-down and bottom-up control.

The processes operating in these calculations are revealed by Fig. 4c and d which show the same calculations carried out for the total phytoplankton abundance over the three months January to March and over April to June. When there is no year-to-year wind variability the GSNW index signal is removed from the spring to early summer period alone. This is a time when, because of density stratification, nutrient stress is important in limiting primary production, which will therefore be enhanced by wind-induced pulses of nutrients across the thermocline.

Removing variability from the cloud has the largest effect on phytoplankton abundance in the winter period but has little effect in the nutrient-limited spring–summer period. Figure 3 shows that the mesozooplankton are dependent on changes in solar irradiance and this implies that mesozooplankton abundance in summer is very dependent on phytoplankton abundance earlier in the year. This is consistent with Colebrook's observation¹⁹ that much of the interannual variability of zooplankton in the North Sea has its origins in winter, with its occurrence through the year being a function of persistence.

The critical process appears to be the control of phytoplankton growth by vertical turbulent mixing in winter, as discussed in ref. 20. Both spring–summer mesozooplankton and winter phytoplankton abundances are strongly correlated with the winter temperature difference between the surface and the bottom (cumulative sum

probabilities 0.002 and 0.000, respectively) even though the mean temperature difference is only 0.07 °C. Corresponding probabilities with the surface temperature are much larger at 0.41 and 0.26. The temperature difference is more correlated with the GSNW index (probability 0.12) than is the surface temperature (0.8).

Even so, there is still an additional effect from summer populations because the mesozooplankton graph, in the absence of wind variability (Fig. 3), shows less similarity to those of the primary producers and bacteria, not having such a clear plateau from 1972 to 1990. This may be part of the reason the mesozooplankton abundance is more strongly correlated with the GSNW index than is the winter temperature difference.

Although it remains unclear what mechanism beyond chance might be responsible for the associations between the atmospheric observations and the GSNW index, we have used the signal as a probe to show how a complex ecosystem can extract information that is scattered throughout a set of meteorological variables. A general consequence of our results is that biological systems can exhibit responses to subtle climatic signals, signals that may be distinct from those that are the most apparent. This could be a significant feature of future responses to climate change. A secondary consequence is the possibility that changes in biological populations could be sensitive indicators of previously unknown climatic processes. Our results also indicate a degree of predictability for summer zooplankton abundance on the basis of knowledge of winter conditions. □

Methods

The GSNW index calculated from the latitude of the north wall of the Gulf Stream close to the coast of the USA^{6,7}. The estimate of total copepods used as a measure of total zooplankton abundance mainly reflects the numerical abundance of smaller zooplankton taxa.

Probabilities of cumulative sums

The test of statistical significance applied to the graphs was designed to determine objectively the likelihood of low, flat regions occurring. It therefore needs to examine both how small is the slope and the length of the flat period, while taking account of serial correlation in the data. In the test used, 2,000 random plankton series were generated, each having the same serial correlation as the observed series. To measure the slope of each of the graphs, a slope was calculated between every pair of points (adjacent and non-adjacent), and these values were averaged. The slope will be less than that of the random line (2) for a positive correlation but can be greater than 2 if the correlation is negative. In order to focus on the probability of low slopes, slopes greater than 2 were excluded from the average. The average slope was then compared with those calculated by applying exactly the same procedure to each of the random plankton series. The number of random series giving a slope at least as small as the average gives an estimate of the probability (*P*) that such a small slope would arise by chance.

ERSEM model

The physical model simulates the vertical density structure and mixing processes throughout the water column. ERSEM describes the biogeochemical cycling of carbon, nitrogen, phosphorus and silicate through the pelagic food web, and has a structure (Fig. 2) which allows it to switch from a mesotrophic ecosystem to one dominated by the microbial loop. It is one of the most complete marine ecosystem models that have been developed.

ERSEM considers the ecosystem to be a series of interacting physical, chemical and biological processes that together exhibit coherent system behaviour. The dynamics of biological functional groups are described by population processes (growth, migration and mortality) and physiological processes (ingestion, respiration, excretion and egestion). The ecosystem is subdivided into three functional types: producers (phytoplankton), decomposers (pelagic bacteria) and consumers (zooplankton).

These broad functional classifications are then subdivided, by grouping biota according to their trophic level (subdivided according to size classes or feeding method) to create a food web (Fig. 2). Physiological processes and population dynamics are described by fluxes of carbon or nutrients between functional groups. It is assumed that whatever compositional changes occur within each pool over time, they are not large enough to cause substantial and persistent errors in the prediction of pool scale rate processes. State variables have been chosen in order to keep the model relatively simple without omitting any component that exerts a significant influence upon the energy balance of the system.

The chemical dynamics of nitrogen, phosphorus, silicate and oxygen are coupled to the biologically driven carbon dynamics. The combination of a food web with coupled nutrient dynamics allows the model to adjust to spatial and temporal variations in carbon and nutrient availability and reproduce the different types of ecosystem behaviour¹⁶.

The phytoplankton pool is described by three functional groups based on size and trophic position²¹: diatoms (20–200 µm), consumed by micro and mesozooplankton;

autotrophic flagellates (2–20 μm), consumed by micro and mesozooplankton; picoplankton (0.2–2 μm), consumed by heterotrophic nanoflagellates; and inedible phytoplankton >20 μm . The uptake of nutrients (NO_3 , NH_4 and PO_4) have been decoupled from the carbon assimilation processes by including dynamic nutrient kinetics²², whereby nutrient uptake is dependent on both the level of intercellular storage and external nutrient concentrations. The microbial food web contains bacteria, heterotrophic flagellates and mesozooplankton, each with dynamically varying C:N:P ratios and is described in ref. 23. Bacteria consume DOC, decompose detritus and can compete for inorganic nutrients with phytoplankton. Heterotrophic flagellates feed on bacteria and picoplankton and are consumed by microzooplankton and mesozooplankton. Microzooplankton feed on diatoms, autotrophic and heterotrophic flagellates and are consumed by mesozooplankton. Mesozooplankton feed on diatoms, autotrophic flagellates and microzooplankton²⁴. All three grazer groups are cannibalistic.

Simulations were made with the ERSEM parameter sets used in ref. 15, for the Humber plume region of the North Sea. The model was forced by heat fluxes calculated from meteorological data observed at Dublin. Although data for Dublin are not from the North Sea, Dublin lies directly in the path of weather systems which commonly move from the Gulf Stream to the North Sea.

Received 25 September 2001; accepted 24 January 2002.

1. Mysterud, A., Stenseth, N. C., Yoccoz, N. G., Langvæn, R. & Steinhel, G. Nonlinear effects of large-scale climatic variability on wild and domestic herbivores. *Nature* **410**, 1096–1099 (2001).
2. Sugihara, G., Grenfell, B. & May, R. M. Distinguishing error from chaos in ecological time series. *Phil. Trans. R. Soc. Lond. B* **330**, 235–251 (1990).
3. Berryman, A. A. & Millstein, J. A. Are ecological systems chaotic—and if not, why not? *Trends Ecol. Evol.* **4**(1), 26–28 (1989).
4. Cane, M. A., Eshel, G. & Buckland, R. W. Forecasting Zimbabwean maize yield using eastern equatorial Pacific sea surface temperature. *Nature* **370**, 204–205 (1994).
5. Shackleton, N. J. The 100,000-year ice-age cycle identified and found to lag temperature, carbon dioxide and orbital eccentricity. *Science* **289**, 1897–1902 (2000).
6. Taylor, A. H., Colebrook, J. M., Stephens, J. A. & Baker, N. G. Latitudinal displacements of the Gulf Stream and the abundance of plankton in the north-east Atlantic. *J. Mar. Biol. Assoc. UK* **72**, 919–921 (1992).
7. Taylor, A. H. North-south shifts of the Gulf Stream and their climatic connection with the abundance of zooplankton in the UK and its surrounding seas. *ICES J. Mar. Sci.* **52**, 711–721 (1995).
8. Glover, R. S. The continuous plankton recorder survey of the North Atlantic. *Symp. Zool. Soc. Lond.* **19**, 189–210 (1967).
9. Frid, C. L. J. & Huluselan, N. V. Far field control of long term changes in Northumberland (NW North Sea) coastal zooplankton. *ICES J. Mar. Sci.* **53**(6), 972–977 (1996).
10. Taylor, A. H. in *Changing States of Large Marine Ecosystems of the North Atlantic* (eds Sherman, K. & Skjoldal, H.-R.) (in the press).
11. George, D. G. The impact of regional-scale changes in the weather on long-term dynamics of *Eudaptomus* and *Daphnia* in Esthwaite Water, Cumbria. *Freshwat. Biol.* **45**, 111–121 (2000).
12. George, D. G. & Taylor, A. H. UK lake plankton and the Gulf Stream. *Nature* **378**, 139 (1995).
13. Hurrell, J. W. Decadal trends in the North Atlantic Oscillation: regional temperatures and precipitation. *Science* **269**, 676–679 (1995).
14. Allen, J. I., Blackford, J. C. & Radford, P. J. A 1-D vertically resolved modelling study of the ecosystem dynamics of the middle and southern Adriatic Sea. *J. Mar. Sys.* **18**, 265–286 (1998).
15. Allen, J. I., Howland, R. M. H., Bloomer, N. & Uncles, R. J. Simulating the spring phytoplankton bloom in the Humber Plume, UK. *Mar. Poll. Bull.* **37**, 295–305 (1999).
16. Baretta, J. W., Ebanhoh, W. & Ruardij, P. (eds) The European regional seas ecosystem model II. *J. Sea Res.* **38**(3/4), 229–483 (1997).
17. Blumberg, A. F. & Mellor, G. L. in *Mathematical Modelling of Estuarine Physics* (Proc. Int. Symp. Hamburg, 1978) (eds Sunderland & Holtz) 203–214 (Springer, Berlin, 1980).
18. Taylor, A. H. North-south shifts of the Gulf Stream: ocean-atmosphere interactions in the North Atlantic. *Int. J. Climatol.* **16**, 559–583 (1996).
19. Colebrook, J. M. Continuous plankton records: overwintering and annual fluctuations in the abundance of zooplankton. *Mar. Biol.* **84**, 261–265 (1985).
20. Huisman, J., van Oostven, P. & Weissing, F. J. Critical depth and critical turbulence: Two different mechanisms for the development of phytoplankton blooms. *Limnol. Oceanogr.* **44**(7), 1781–1787 (1999).
21. Ebenhöh, W., Baretta, J. W. & Baretta-Bekker, J. G. The primary production module in a marine ecosystem model ERSEM II. *J. Sea Res.* **38**, 173–194 (1997).
22. Droop, M. R. The nutrient status of algal cells in continuous culture. *J. Mar. Biol. Assoc. UK* **54**, 825–855 (1974).
23. Baretta-Bekker, J. G., Baretta, J. W., Hansen, A. S. & Riemann, B. An improved model of carbon and nutrient dynamics in the microbial food web in marine enclosures. *Aquat. Microb. Ecol.* **14**, 91–108 (1998).
24. Broekhuizen, N. R., Heath, M. R., Hay, S. G. & Gurney, S. C. Modelling the dynamics of the North Sea's mesozooplankton. *Neth. J. Sea Res.* **33**, 381–406 (1995).

Acknowledgements

We wish to thank J. Stephens and J. Dearman for assisting with the calculations. B. Clarke provided statistical advice. A.H.T. is a Fellow of the Sir Alister Hardy Foundation for Ocean Science, which provided the plankton data. This work is part of the Core Strategic Programme of Plymouth Marine Laboratory.

Competing interests statement

The authors declare that they have no competing financial interests.

Correspondence and requests for materials should be addressed to A.H.T. (e-mail: aht@pml.ac.uk).

Direct visuomotor transformations for reaching

Christopher A. Buneo, Murray R. Jarvis, Aaron P. Batista* & Richard A. Andersen

Division of Biology, California Institute of Technology, Mail Code 216-76, Pasadena, California 91125, USA

The posterior parietal cortex (PPC) is thought to have a function in the sensorimotor transformations that underlie visually guided reaching, as damage to the PPC can result in difficulty reaching to visual targets in the absence of specific visual or motor deficits¹. This function is supported by findings that PPC neurons in monkeys are modulated by the direction of hand movement, as well as by visual, eye position and limb position signals^{2–9}. The PPC could transform visual target locations from retinal coordinates to hand-centred coordinates by combining sensory signals in a serial manner to yield a body-centred representation of target location^{10–12}, and then subtracting the body-centred location of the hand. We report here that in dorsal area 5 of the PPC, remembered target locations are coded with respect to both the eye and hand. This suggests that the PPC transforms target locations directly between these two reference frames. Data obtained in the adjacent parietal reach region (PRR) indicate that this transformation may be achieved by vectorially subtracting hand location from target location, with both locations represented in eye-centred coordinates.

The problem that we address here is shown in Fig. 1a. Although the execution of movement requires the specification of a detailed pattern of inputs to the muscles, movement planning is believed to involve the computation of higher level movement parameters, such as the direction and/or distance that the hand must move to reach the target (vector M)¹⁰. This is due to the fact that movement goals, as well as evidence of our success in achieving these goals, are largely expressed in high level terms, that is, as visually perceived discrepancies between the position of the hand and target or deviations from a desired path¹³. Hereafter we use the term 'target position in hand coordinates' to describe vector M in Fig. 1a, although the terms 'movement vector' and 'motor error' could also be used. This information could be derived by subtracting the sensed location of the hand (vector H) from the sensed location of the target (vector T), as long as hand position and target position are coded in a common frame of reference. However, although target position appears to be coded in eye-centred (retinal) coordinates in the early stages of reach planning¹⁴, hand position is derived from both visual and proprioceptive signals, and can conceivably be coded in eye-centred coordinates, body centred coordinates (that is, with respect to the torso), or both. It is unclear therefore whether the operation shown in Fig. 1a is achieved by subtracting the position of the hand from the position of the target directly, using eye-centred coordinates (Fig. 1a, b), or by transforming target locations from eye- to head- to body-centred coordinates, and then subtracting the body-centred position of the hand^{10,11} (Fig. 1c).

We have approached this problem by analysing the reach-related activity of neurons in the PPC, while varying target position, hand position and gaze direction. Single cell recordings were obtained from area 5 (Fig. 2a, b), a subdivision of the PPC that projects directly to cortical and subcortical motor structures^{15–17}. In an initial experiment, 89 neurons from two monkeys were studied under four experimental conditions (Fig. 2c). In two conditions, gaze was held constant at the centre position of a vertically oriented

* Present address: Howard Hughes Medical Institute, and Department of Neurobiology, Stanford University School of Medicine, Fairchild Building, Room D209, Stanford, California 94305, USA